# SPE SPE-169040-MS

# Adsorption of a Switchable Cationic Surfactant on Natural Carbonate Minerals

Leyu Cui, Kun Ma[1], Rice University; Ahmed A. Abdala, Petroleum Institute University; Lucas J. Lu, Ivan Tanakov, Sibani L. Biswal and George J. Hirasaki, Rice University
1 current affiliation: Total E&P Research and Technology USA, LLC



This paper was prepared for presentation at the SPE Improved Oil Recovery Symposium held in Tulsa, Oklahoma, USA, 12–16 April 2014.



## Abstract

A switchable cationic surfactant, *e.g.*, tertiary amine surfactant Ethomeen C12, has been previously described as a surfactant that can be injected in high pressure $CO_2$ for foam mobility control. C12 can dissolve in high pressure $CO_2$ as a nonionic surfactant and equilibrate with brine as a cationic surfactant. Here we describe the adsorption characteristics of this surfactant in carbonate formation materials. The adsorption of this surfactant is sensitive to the equilibrium pH, the electrolyte composition of the brine, and the minerals in carbonate formation materials.

Pure C12 is a nonionic surfactant. When it is mixed with brine, the solution has high pH and limited solubility. However, when the surfactant solution in brine is equilibrated with high pressure $CO_2$, the pH is about 4, the surfactant switches to a cationic surfactant and becomes soluble. Thus the adsorption is also a function of pH. The adsorption of C12 on calcite at low pH is low, *e.g.*, 0.5 mg/m$^2$. However, if the carbonate formation contains silica or clays, the adsorption is high, as is typical for cationic surfactants. The adsorption of C12 on silica decreases with increase in divalent ($Ca^{2+}$ and $Mg^{2+}$) and trivalent ($Al^{3+}$) cations. This is due to the competition for the negatively charged silica sites between the multivalent cations and the monovalent cationic surfactant. An additional effect of the presence of divalent cations in the brine is that it reduces the dissolution of calcite or dolomite in presence of high-pressure $CO_2$. The dissolution of calcite and dolomite is harmful because of formation damage and increased alkalinity. The latter raises the pH and thus increases adsorption of C12 or even cause surfactant precipitation.

## Introduction

The oil recovery efficiency in $CO_2$ flooding process is enhanced with pressure, especially when higher than the minimum miscible pressure (MMP) (Hao, et al., 2004; Shedid, et al., 2007; Sequeira, et al., 2008). But the low viscosity and density of the injected $CO_2$ often result in the poor mobility control and instability of the displacement front, which results in the low sweep efficiency and gravity override problems (Hanssen and Surguchev, 1994). $CO_2$ foam is a promising way to solve these problems

and has been extensively investigated in both laboratory and field studies recently (Moradi-Araghi, et al., 1997; Farajzadeh, et al., 2010; Chen, et al., 2014; Talebian, et al., 2013; Stephenson, et al., 1993; Stevens, et al., 1995; Sanders, et al., 2012). In the $CO_2$ foam flooding process, surfactants are usually used as foaming agents (Farajzadeh, et al., 2010; Chen, et al., 2014). However the surfactant adsorption on the minerals detrimentally affects the foam mobility control, because the foam strength decreases with surfactant concentrations (Tsau and Heller, 1992), and is comparative to the water-gas injection after the concentrations fall below a threshold value (Liu, et al., 2005). Extra surfactants should be injected to compensate the surfactants adsorption on the rocks, which results in the increase of cost for foam flooding process. Thus, the surfactant adsorption should be investigated and reduced to an acceptable value in foam process.

The electrostatic force is a determining factor during the surfactants adsorption process (Zhang and Somasundaran, 2006). Therefore, the electrokinetics properties of mineral surfaces, *i.e.*, the surface charge and zeta potential, are the important parameters for selecting surfactants for chemical-enhanced oil recovery process. Generally, the sign of zeta potential is the same as that of surface charge, the magnitude of zeta potential is affected by electrolyte. The adsorption of the anionic surfactants is usually lower than that of cationic surfactants on silica ($SiO_2$) minerals (Thibaut, et al., 2000; Ma, et al., 2013), because of the negative surface charge (Kosmulski, 2003; Mannhardt, et al., 1993) at pH higher than 4. The clay minerals, *e.g.*, kaolinite, bear both positive and negative surface charges because of the heterogeneity of the structures (Tombácz and Szekeres, 2006), which results in the capacity to adsorb both anionic and cationic surfactants (Sánchez-Martín, et al., 2008). However, the adsorption of cationic surfactants on clays is higher, owning to the net negative surface charge in a wide pH range (Alkan, et al., 2005). The surface charge of carbonate minerals, *e.g.*, calcite and dolomite, in water are positive at pH lower than about 9 (Somasundaran and Agar, 1967; Pokrovsky, et al., 1999). But the surface charge of carbonate minerals can be changed with the concentrations of potential determining ions, *i.e.*, $CO_3^{2-}$ and $Me^{2+}$ ($Ca^{2+}$ and $Mg^{2+}$) (Heberling, et al., 2011), and become negative at neutral pH in the presence of carbonate/bicarbonate ions (Hirasaki and Zhang, 2004). The higher concentrations of $Me^{2+}$ lead a more positive surface charge, and the higher concentration of $CO_3^{2-}$ leads a more negative surface charge (Foxall, et al., 1979). Here, we demonstrate the surface charges of carbonate minerals are positive at reservoir conditions during $CO_2$ flooding, *i.e.*, in the injected or formation brine and presence of high pressure $CO_2$. And, the low adsorption of a switchable cationic surfactant on a pure calcite mineral at 2 atmosphere $CO_2$ also supports our analysis of surface charge.

The switchable cationic surfactant, *i.e.*, ethoxylated amine C12 (C12), has been reported as a good $CO_2$ foam agent at high temperature, pressure and salinity (Chen, et al., 2014). The adsorption of the C12 surfactant on various minerals was measured. The results show that the adsorption was low as 0.47 mg/m$^2$ on the pure carbonate mineral, but significantly increased to 2.21 mg/m$^2$ on the natural carbonate mineral. That's because the significant amount of negatively charged impurities exist in the natural carbonate minerals, as shown in X-ray photoelectron spectroscopy (XPS) analysis results (Vdović, 2001; Ma, et al., 2013). And the high adsorption of C12 on pure silica and clays reported in this paper further supports above conclusions. The adsorption of cationic surfactants on these negatively charged impurities can be reduced by multivalent cations, *e.g.*, $Mg^{2+}$, $Ca^{2+}$ and $Al^{3+}$, because of the competition of monovalent surfactant and multivalent cations on the negative binding sites. Our results show that the effectiveness of the cations for reducing the adsorption ranges in the order of $Al^{3+}$>$Ca^{2+}$>$Mg^{2+}$, and the adsorption of C12 on silica was reduced from 5.33 mg/m$^2$ in DI water to 3.31 mg/m$^2$ in synthetic brine with $1.51\times10^{-3}$ mol/L $Al^{3+}$.

## Experimental

**Materials**

Ethomeen C12 (C12, AkzoNobel Co.) is a tertiary amine surfactant with one coco alkyl group (mixture from C6 to C18 alkyl chains) and two EO branches with the structure shown in Figure 1. The switchable cationic surfactant, *i.e.*, C12, is a nonionic surfactant at neutral and high pH, and is switched to a cationic surfactant at low pH because of the protonation of the tertiary amine.

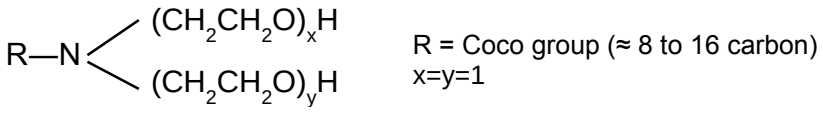


Figure 1 the structure of ethoxylated amine C12

A sodium lauryl ether sulfate surfactant, *i.e.*, STEOL CS-330 (SDES, Stepan Co.), was used as an anionic titrant instead of the traditional titrant, *i.e.*, sodium dodecyl sulfate (SDS), because SDS will precipitate in the high salinity brine, especially in the presence of multivalent ions (Sammalkorpi, et al., 2009). SDES with three ethylene oxide (EO) groups can tolerate the high salinity brine.

The adsorption of C12 was measured on four minerals as shown in Table 1. The surface chemistry of the minerals analyzed by X-ray Photoelectron Spectroscopy (PHI Quantera XPS, Physical Electronics Inc.) has been reported by Ma, et al. (2013) shown in Figure 2. The calcite, kaolin and silica ($SiO_2$) sands are pure minerals and contain negligible impurities. But the dolomite sands contain silicate and aluminum impurities. The distribution of silicate impurity on the whole dolomite surface was scanned by energy dispersive spectroscopy (EDAX, FEI Quanta 400) shown in Figure 3.

Table 1 The list of the minerals (Ma, et al., 2013)

| Name | BET Surface Area ($m^2/g$) | Size (μm) | Resource | Preparation |
|---|---|---|---|---|
| Dolomite | 0.97 | ≤74 | Car Pool Co. | sieved through 200 mesh screen |
| Calcite | 1.67 | 5 | Alfa Aesar | N/A |
| Silica | 1.16 | ≤10 | US Silica Co. | washed with 1 mol/L HCl, 0.01 mol/L $NaHCO_3$ and deionized water sequentially to remove the metal ions in original sands |
| Kaolin | 26.61 | 0.1-4 | Sigma-Aldrich | N/A |

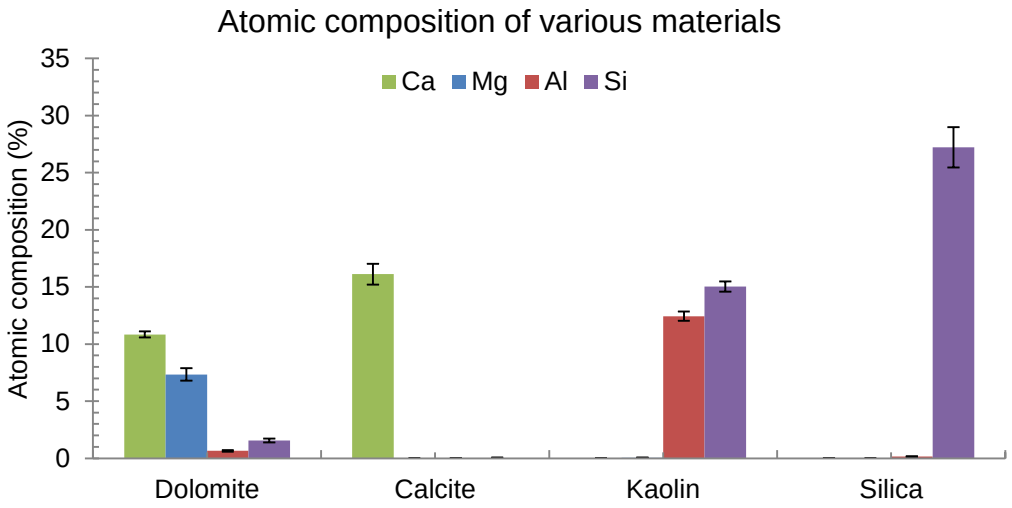


Figure 2 X-ray Photoelectron Spectroscopy (XPS) analysis results of sands (Ma, et al., 2013)

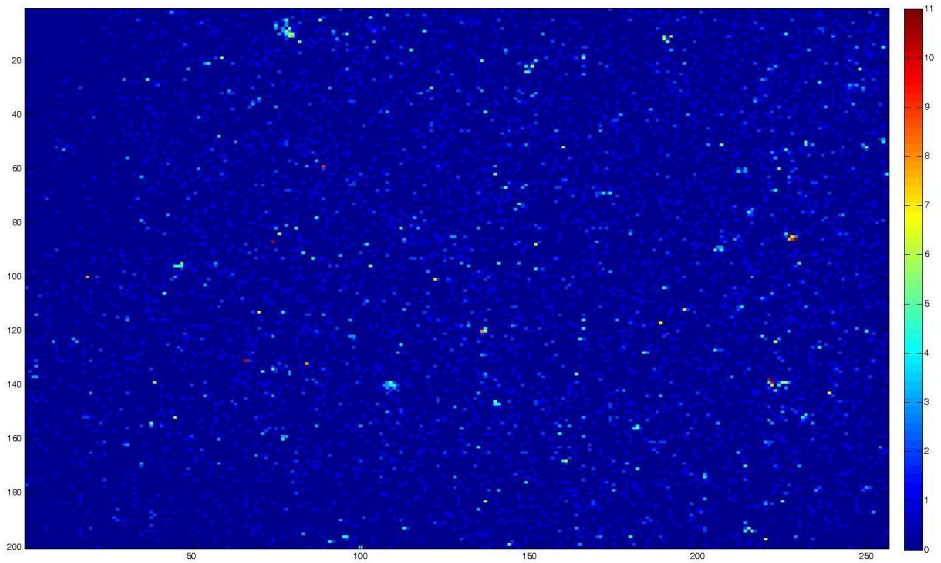

Figure 3 Energy dispersive spectroscopy scan of natural dolomite surface. The blue color is the carbonate surface background; other colored spots are the silica impurity. The strength of silica response increases from blue to red color.

A synthetic brine with 22% total dissolved solid (TDS) was prepared in deionized water (DI water) with the compositions of 182.31 g/L NaCl (catalog # 3624-01, Avantor Performance Materials), 77.25 g/L $CaCl_2 \cdot 2H_2O$ (catalog # 223506, Sigma-Aldrich Co.) and 25.62 g/L $MgCl_2 \cdot 6H_2O$ (catalog # M33, Fisher Scientific Co.).

**Procedure**

**Improved Methylene Blue (MB) Two-Phase Titration with Colorless End Point**

The C12 concentration is determined by an improved MB two-phase titration. The MB solution contains 0.03 g/L methylene blue hydrate (catalog # 66720, Sigma-Aldrich Co.), 5.52 g/L KCl and 126 ml/L HCl (1 mol/L, catalog # HC253654, EMD Millipore Co.). A glass vial (22 ml capacity, catalog # 71000-180, VWR International Co) was used to contain 5.0 ml chloroform, 2.0 ml MB solution and the C12 sample. The anionic titrant of SDES was added in vial by burette (10 ml capacity, 0.02 ml tolerance, catalog # 0370125A, Fisher Scientific Co.). The vial was vigorously shaken after adding titrant and was centrifuged at 3000 rpm for 1-3 minutes to separate the two phases. The blue color is eventually transferred from upper aqueous phase to lower chloroform phase with adding SDES titrant, based on the reactions shown below:

$$C12(aqu.) + H^{+}(aqu.) \leftrightarrow [H \bullet C12]^{+}(aqu.) \ldots\ldots\ldots\ldots\ldots\ldots\ldots\ldots\ldots\ldots Reaction\ 1$$

$$SDES^{-}(aqu.) + [H \bullet C12]^{+}(aqu.) \leftrightarrow [SDES \bullet H \bullet C12](chl.) \ldots\ldots\ldots\ldots Reaction\ 2$$

$$SDES^{-}(aqu.) + MB^{+}(aqu.) \leftrightarrow [Anionic \bullet MB](chl.) \ldots\ldots\ldots\ldots\ldots\ldots Reaction\ 3$$

* $aqu.$ indicates the aqueous phase, $chl.$ indicates the chloroform phase

A spectrophotometer (Genesy 10S UV-vis, catalog # 840-208100, Fisher Scientific Co.) was used to monitor the color change of the aqueous phase. When the light absorbance of the aqueous phase at the characteristic wavelength of MB, *i.e.*, λ=655 nm, fells below 0.04, the aqueous phase is considered to be colorless and the titration reaches the end point.

**Static Adsorption Measurement at 2 atm $CO_2$**

The C12 at neutral and higher pH is sparingly soluble in water, but can be dissolved into $CO_2$ phase. C12 can be protonated to a water soluble cationic surfactant in water or brine at pH lower than 6, as shown in Figure 4. The cloud point of the C12 surfactant in brine increases with decreasing pH, and can be enhanced above 120°C at pH=4.

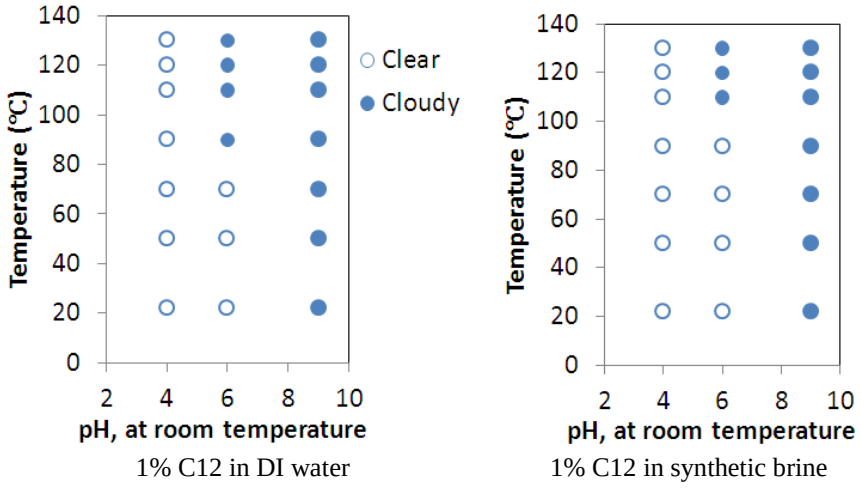


Figure 4 the cloud point of C12 at various pH. The pH is adjusted by HCl.

Acid solutions can't be used to decrease the pH of C12 solution in the adsorption measurements, because the acids will react with carbonate minerals, which results in the increase of pH and loss of the carbonate minerals. $CO_2$ can decrease the pH of aqueous solution by generating carbonic acid and forming a buffer with carbonate minerals to maintain a stable pH of the system. The equilibrium pH of aqueous solutions, $CO_2$ and various minerals can be calculated by PHREEQC software (de Souza and Fjelde, 2013). The results in Figure 5 demonstrate that the equilibrium pH at 2 atmosphere pressure of $CO_2$ is lower than 6, which indicates the C12 solutions can keep clear during the adsorption measurement at room temperature and 2 atmosphere pressure of $CO_2$.

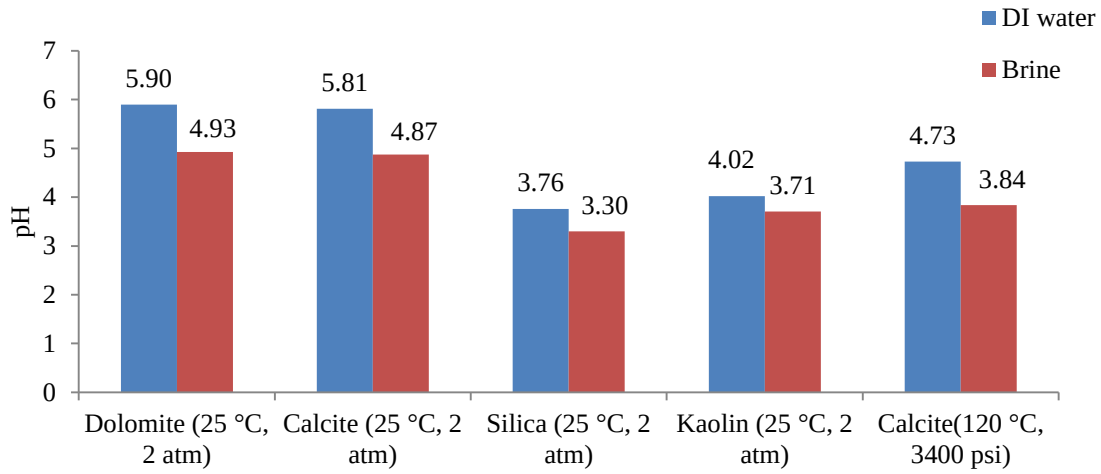


Figure 5 the equilibrium pH of aqueous phase with various minerals, calculated with PHREEQC software. Equilibrium temperature and $CO_2$ pressure are in brackets.

Thus, a static adsorption process at 2 atmosphere $CO_2$ is designed as below: $CO_2$ was injected on the top of a C12 solution to obtain the clear solution at 1 atmosphere pressure. The initial concentration of the C12 solution was determined by the MB two-phase titration. The C12 solution and mineral sand were loaded in a 50 ml stainless steel sample cylinder (item # HSSC15-1BA, Myers & Co. Inc). $CO_2$ at 5 atmospheres (absolute pressure) was injected in the sample cylinder, and then was released to one atmosphere to purge the air out of the cylinder. The residual air fraction was reduced to $(\frac{1}{5})^5 = \frac{1}{3125}$ after the above step was repeated for 5 times. Finally, 2 atmospheres (absolute pressure) $CO_2$ was injected in the cylinder. The cylinder was shaken for 24 hours to reach the adsorption equilibrium, and then stood overnight to roughly separate the liquid and solid mineral. The upper layer of the liquid was withdrawn and was centrifuged at 8,000 rpm for 30 minutes. The supernatant was titrated by MB two-phase titration to determine the residual C12 concentration. The adsorption can be calculated based on following Equation 1:

$$adsorption\left({}^{mg}/_{m^2}\right) = \frac{\left(C_{initial} - C_{residual}\left({}^{mol}/_{g}\right)\right) \times m_{C12}\,(g) \times MW\left({}^{g}/_{mol}\right) \times 1000\left({}^{mg}/_{g}\right)}{m_{sand}\,(g) \times A_{sand}(m^2/g)} \quad Equation\ 1$$

where, $C_{initial}$ and $C_{residual}$ are the initial and residual concentration of C12 solutions; $m_{C12}$ and $m_{sand}$ are the mass of C12 solution and sands loaded in the cylinder; $MW$ is the molecular weight of C12, *i.e.*, 288 g/mol reported by Akzo Nobel Co. $A_{sand}$ is the BET surface area of the sand.

## Results and Discussion

### Surface Charge of Carbonate Minerals

#### Calcite-$H_2O$-$CO_2$

$Me^{2+}$ ($Ca^{2+}$ and $Mg^{2+}$) and $CO_3^{2-}$ are assumed to be the potential determining ions of surface charge for carbonate minerals, *i.e.*, calcite and dolomite (Somasundaran and Agar, 1967; Heberling, et al., 2011). The higher concentrations of $Me^{2+}$ lead more positive surface charge, and the higher concentration of $CO_3^{2-}$ leads more negative surface charge. The reactions listed in Table 2 exist in a carbonate, *e.g.*, calcite, -$CO_2$-$H_2O$ system (Ma, et al., 2013). There are 9 species constrained by 5 reactions in three phases, and the surface charge is considered as another variable which is constrained by concentrations of potential determining ions. Thus, the total freedom of the system is 3. At a fixed temperature, the concentrations of potential determining ions are functions of two arbitrary variables, *i.e.*, pH and partial pressure of $CO_2$, expressed in Equation 2 and 3.

$$[Ca^{2+}] = \frac{K_{sp}[H^+]^2}{K_1 K_2 K_H P_{CO_2}} \qquad Equation\ 2$$

$$[CO_3^{2-}] = \frac{K_1 K_2 K_H P_{CO_2}}{[H^+]^2} \qquad Equation\ 3$$

At a fixed temperature and zero surface charge (zeta potential=0), the system depends on only one variable, *i.e.*, the pH is determined by the partial pressure of $CO_2$ as well. This can be demonstrated by the data of Heberling, et al. (2011). They reported the linear relationship between pH and $\log(P_{CO_2})$ at the condition of zero zeta potential in low ionic strength solutions with empirical regression: $\log(P_{CO_2})$= -1.71 pH+11.2, which implies the ratio $\frac{P_{CO_2}}{[H^+]^{1.71}}$ equals to $1.6\times10^{11}$. Thus, the potential determining ions concentrations can be calculated as expressed in Equation 4 and 5 at zero zeta potential and 25 °C. Note that the potential determining ion concentration at the condition of zero zeta potential is denoted with the superscript (*).

$$[Ca^{2+}]^* = \frac{K_{sp}\ (P_{CO_2})^{0.17}}{1.3\times10^{13} K_1 K_2 K_H} \qquad Equation\ 4$$

$$[CO_3^{2-}]^* = \frac{1.3\times10^{13} K_1 K_2 K_H}{(P_{CO_2})^{0.17}} \qquad Equation\ 5$$

The Equations 4 and 5 illustrate the potential determining ions concentrations at 25 °C and zero zeta potential are proportional to $(P_{CO_2})^{0.17}$ or $\frac{1}{(P_{CO_2})^{0.17}}$, respectively, and can be assumed nearly a constant for $P_{CO_2}$ higher than 1 atm, as demonstrated in Figure 6. This observation states that the concentrations of the potential determining ions are approximately constant for the condition of zero zeta potential for a given temperature even though the $CO_2$ pressure may vary widely. Furthermore, inspection of Equations 4 and 5 shows that the carbonate ion concentration at the condition of zero zeta potential is not independent of the

calcium concentration. This is also recognized from the solubility product constraint. Thus only the calcium concentration is needed to specify the condition of zero zeta potential at a given temperature. This quantity may be called the isoelectric calcium concentration, $[Ca^{2+}]^*$. The utility of this simplification is that if the calcium concentration of the brine is greater than the isoelectric calcium concentration, then the zeta potential should be positive; and if the calcium concentration of the brine is less than the isoelectric calcium, then the zeta potential should be negative. Generally the sign of the surface charge is the same as that of the zeta potential.

Table 2 The reactions and equilibrium constants of calcite-$CO_2$-$H_2O$ system at 25 C and low ionic strength (activity coefficient=1), (Ma, et al., 2013)

| Reaction | Equilibrium Constant | -$\log_{10}$(K) at 25 °C |
|---|---|---|
| $CaCO_3(s) \leftrightarrow Ca^{2+} + CO_3^{2-}$ | $K_{sp} = [Ca^{2+}][CO_3^{2-}]$ | 8.42 |
| $CO_2\ (g) + H_2O\ (l) \leftrightarrow H_2CO_3$ | $K_H = \frac{[H_2CO_3]}{P_{CO_2}}$ | 1.47 |
| $H_2CO_3 \leftrightarrow H^+ + HCO_3^-$ | $K_1 = \frac{[H^+][HCO_3^-]}{[H_2CO_3]}$ | 6.35 |
| $HCO_3^- \leftrightarrow H^+ + CO_3^{2-}$ | $K_2 = \frac{[H^+][CO_3^{2-}]}{[HCO_3^-]}$ | 10.33 |
| $H_2O\ (l) \leftrightarrow H^+ + OH^-$ | $K_W = [H^+][OH^-]$ | 14.0 |

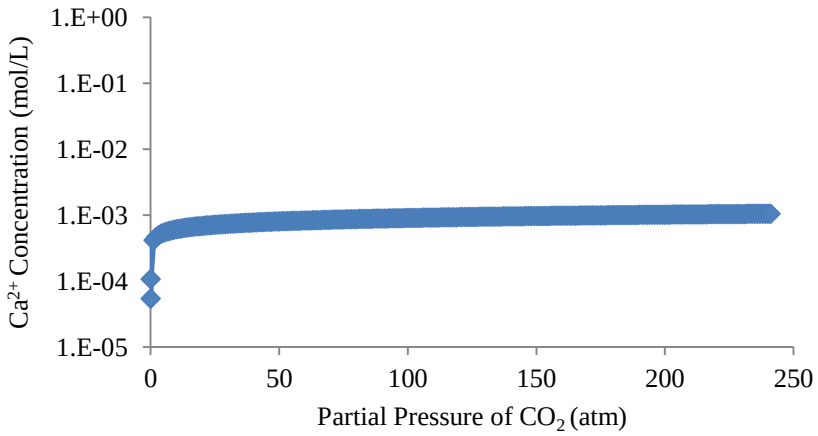


Figure 6 The $Ca^{2+}$ concentrations at zero zeta potential and 25 °C at various partial pressure of $CO_2$, calculated from Equation 4.

**Dolomite-$H_2O$-$CO_2$**

Dolomite-$H_2O$-$CO_2$ system contains one more potential determining ion, *i.e.*, $Mg^{2+}$, but the reaction is still 5, as listed in Table 3, which results the total freedom degree is 4. At a given temperature and zero zeta potential, the freedom degree is 2, which indicates that the pH and partial pressure of $CO_2$ can be independent variables. The similar relationship between pH and $P_{CO2}$ in Calcite- $H_2O$-$CO_2$ system does not exist in Dolomite-$H_2O$-$CO_2$ system. The isoelectric concentration of calcium and magnesium depends on both pH and $P_{CO2}$. The similar relationship in Figure 6 can't be archived for dolomite. However, Pokrovsky, et al. (1999) has measured the zeta potential data at various calcium and magnesium activities, from which similar interpretation for dolomite zeta potential may be possible. The measured isoelectric calcium and magnesium activities at zero zeta potential, respectively, *i.e.*, $a^*_{Ca^{2+}}$=3.16×10$^{-4}$ mol/L and $a^*_{Mg^{2+}}$=6.31×10$^{-4}$ mol/L.

Table 3 The reactions and equilibrium constants of dolomite-$CO_2$-$H_2O$ system at 25 °C and low ionic strength (activity coefficient=1) (Ma, et al. 2013; Hyeonga and Capuano, 2001)

| Reaction | Equilibrium Constant | -log$_{10}$(K) at 25 °C |
|---|---|---|
| $CaMg(CO_3)_2 \leftrightarrow Ca^{2+} + Mg^{2+} + CO_3^{2-}$ | $K_{sp} = [Ca^{2+}][Mg^{2+}][CO_3^{2-}]^2$ | 16.9 |
| $CO_2\ (g) + H_2O\ (l) \leftrightarrow H_2CO_3$ | $K_H = \frac{[H_2CO_3]}{P_{CO_2}}$ | 1.47 |
| $H_2CO_3 \leftrightarrow H^+ + HCO_3^-$ | $K_1 = \frac{[H^+][HCO_3^-]}{[H_2CO_3]}$ | 6.35 |
| $HCO_3^- \leftrightarrow H^+ + CO_3^{2-}$ | $K_2 = \frac{[H^+][CO_3^{2-}]}{[HCO_3^-]}$ | 10.33 |
| $H_2O\ (l) \leftrightarrow H^+ + OH^-$ | $K_W = [H^+][OH^-]$ | 14.0 |

**High salinity brine**

In high salinity brine, activity of $Me^{2+}$ is more reasonable to be used to determine the surface charge. The activity of $Ca^{2+}$ and $Mg^{2+}$ ions in our tests calculated with PHREEQC (version 3.0.2) software are compared with the $Me^{2+}$ concentrations and activities at zero zeta potential, as listed in Table 4. The activities in both DI water and brine are higher than the concentrations and activities at zero surface charge, which indicates that the surface charges of carbonate minerals were positive in the

adsorption measurement.

Table 4 $Me^{2+}$ activities and isoelectric concentrations during adsorption tests on carbonate minerals

| $CO_2$ pressure (atm) | Sand | Solvent | Activity in Electrolyte of Adsorption Measurement | | Concentrations or activities at zero zeta potential | |
|---|---|---|---|---|---|---|
| | | | $a_{Ca^{2+}}$ (mol/L) | $a_{Mg^{2+}}$ (mol/L) | $[Ca^{2+}]^*$ / $a^*_{Ca^{2+}}$ (mol/L) | $[Mg^{2+}]^*$ / $a^*_{Mg^{2+}}$ (mol/L) |
| 2 | Calcite | DI water | $5.6\times10^{-3}$ | 0 | $4.7\times10^{-4}$ | 0 |
| 2 | Calcite | Synthetic Brine | $5.0\times10^{-1}$ | $2.2\times10^{-1}$ | $4.7\times10^{-4}$ | 0 |
| 2 | Dolomite | DI water | $3.2\times10^{-3}$ | $3.3\times10^{-3}$ | $3.16\times10^{-4}$ | $6.31\times10^{-4}$ |
| 2 | Dolomite | Synthetic Brine | $5.0\times10^{-1}$ | $2.2\times10^{-1}$ | $3.16\times10^{-4}$ | $6.31\times10^{-4}$ |

**Adsorption of C12 on Pure and Natural Carbonates**

The adsorption of C12 in DI water and brine were measured on pure and natural carbonate minerals, respectively. The Langmuir type isotherm curves of C12 adsorption are shown in Figure 7. The adsorption curves reach their plateaus at about 0.1% (wt) residual concentration. An average of the adsorption on the plateaus was taken as the equilibrium adsorption in flooding process shown in Figure 8, because of the high surfactant concentration in $CO_2$ foam flooding (Chen, et al., 2014).

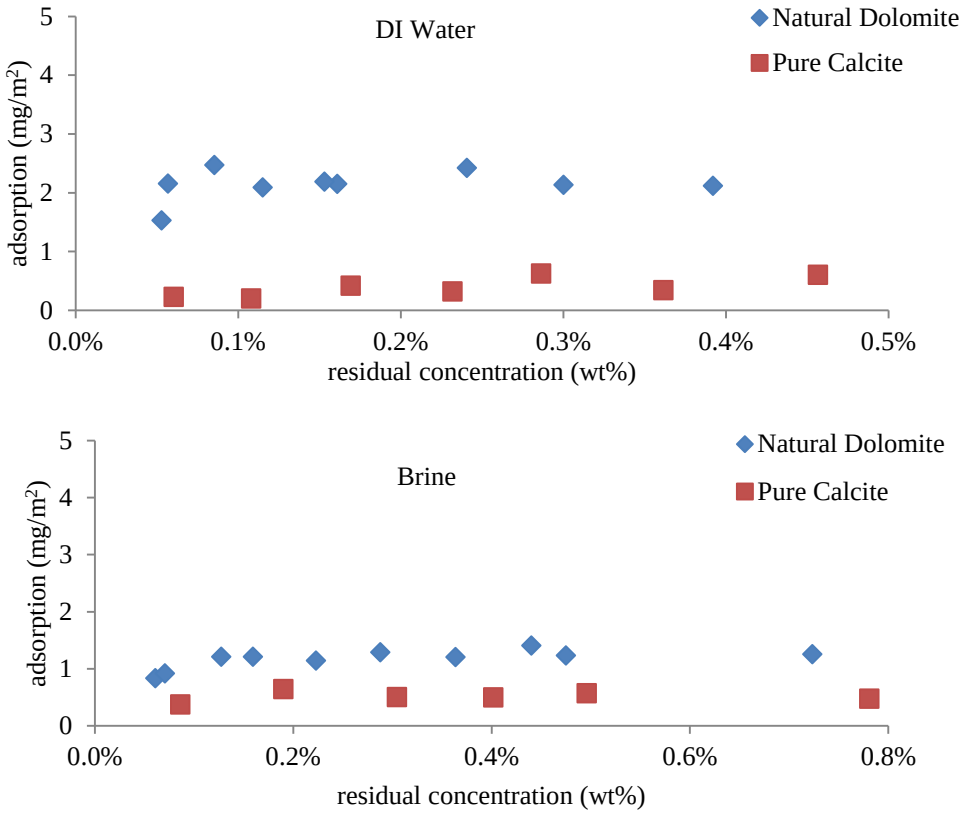


Figure 7 the adsorption curves of C12 in DI and Brine on both natural dolomite and pure calcite

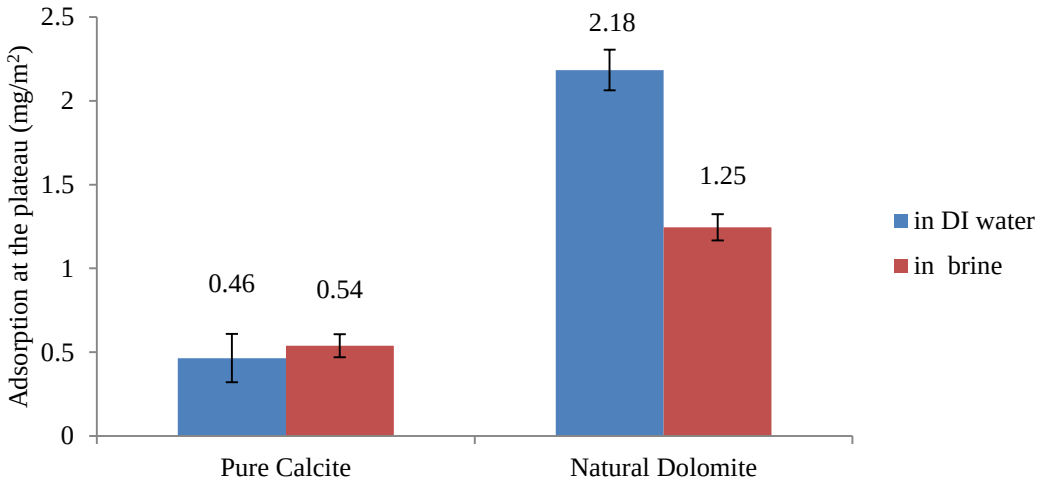


Figure 8 the equilibrium adsorption of C12 in different solutions on carbonate minerals

The results in Figure 8 reveal that the adsorption on the pure calcite, *i.e.*, 0.46 mg/m$^2$ in DI water and 0.54 mg/m$^2$ in synthetic brine, was lower than that on natural dolomite, *i.e.*, 2.18 mg/m$^2$ in DI water and 1.25 mg/m$^2$ in synthetic brine, owning to the high adsorption of C12 on negatively charged impurities on natural dolomite surface (Figure 3). Thus, the adsorption can be significant for cationic surfactant used in natural carbonate reservoirs which contains the negatively charged impurities. Similar results were reported by Tabatabal, et al. (1993) and Ma, et al. (2013) for dodecylpyridinium chloride (DPC) and

hexadecylpyridinium chloride (CPC) in DI water, respectively. However, the adsorption of permanent cationic surfactants, *i.e.*, DPC and CPC, on pure calcite reported by Tabatabal, et al. (1993) and Ma, et al. (2013) is very small and much lower than that of switchable cationic surfactant, *i.e.*, C12. This may be because only a portion of C12 is protonated at the tested pH (Figure 5), and the other portion is nonionic surfactants which cause the relatively high adsorption compared to permanent cationic surfactants. Note that the cloud point pH at elevated temperature in Figure 4 is somewhere between pH 4 and 6. The brine pH in our adsorption experiments with carbonate minerals were somewhere between pH 4 and 6, Figure 5. In $CO_2$ flooding, the equilibrium pH under reservoir conditions is lower (Figure 5) which implies the larger ratio of cationic to nonionic C12 surfactant and possibly less adsorption on pure calcite.

**The Influence of Cations on Adsorption**

The adsorption of C12 on natural carbonate minerals can be reduced by adding multivalent cations, *i.e.*, $Mg^{2+}$, $Ca^{2+}$ and $Al^{3+}$.

The adsorption of C12 on dolomite minerals in synthetic brine were lower than that in DI water as shown in Figure 8, because of the competition of the cations and C12 surfactant on the negative binding sites.

The adsorption of C12 in NaCl and $MgCl_2$ solutions with the same ionic strength as the synthetic brine (Table 5) were tested to investigate the influence of various cations. $CaCl_2$ solution wasn't prepared, because $Ca^{2+}$ will precipitate at 2 atm $CO_2$ at such high ionic strength.

Table 5 Cations concentration of various solutions

| | Brine | NaCl | $MgCl_2$ |
|---|---|---|---|
| $Al^{3+}$ (mol/L) | 0 | 0 | 0 |
| $Ca^{2+}$ (mol/L) | $5.25\times10^{-1}$ | 0 | 0 |
| $Mg^{2+}$(mol/L) | $1.26\times10^{-1}$ | 0 | 1.69 |
| $Na^{+}$ (mol/L) | 3.12 | 5.08 | 0 |
| Ionic Strength (mol/L) | 5.08 | 5.08 | 5.08 |

Tabatabal, et al. (1993) attributed the reduction of adsorption by multivalent cations to the increase of surface charge by lattice ions ($Ca^{2+}$ and $Mg^{2+}$), rather than the competition of cations and cationic surfactants. Thus, the adsorption on pure silica and kaolin was also tested. The divalent cations are not lattice or potential determining ions for silica ($SiO_2$) and kaolin, and yet can reduce the adsorption of C12 as well as for natural dolomite, shown in Figure 9.

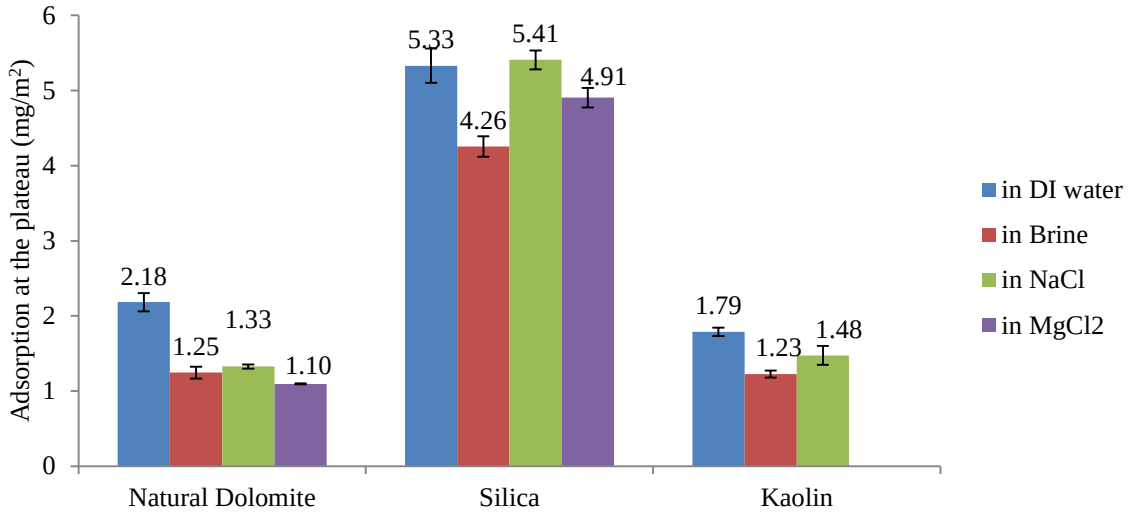


Figure 9 The adsorption of C12 on natural dolomite, pure silica and kaolin in various solutions

The adsorption on dolomite, silica ($SiO_2$) and kaolin in brine is lower than that in DI water, which indicates the cations in brine can reduce the adsorption on the negative binding sites. But the adsorption on silica in NaCl solution is close to that in DI water, which discloses the monovalent cation, *i.e.*, $Na^+$, does not affect the adsorption of C12 on silica. The adsorption on silica in $MgCl_2$ solution is lower than that in DI water, and is higher than that in brine, which reveals that $Mg^{2+}$ can reduce the adsorption, but is not as effective as $Ca^{2+}$. The different influence of $Mg^{2+}$ and $Ca^{2+}$ on the adsorption is caused by the diameters of their hydrated cations. The hydrated $Mg^{2+}$ of 0.8 nm diameter is larger than the hydrated $Ca^{2+}$ of 0.6 nm diameter in aqueous solutions, which results in the weaker electric potential of $Mg^{2+}$ (Kielland, 1937).

However, the adsorption on dolomite and kaolin in NaCl and $MgCl_2$ solutions are lower than those in DI water and are close to those in brine. That's because the concentrations of multivalent cations in NaCl and $MgCl_2$ solution are one order of magnitude higher than those in DI water, calculated by PHREEQC software listed in Table 6 and 7. Additionally, the natural dolomite may contain clays which can bring more $Al^{3+}$ in NaCl and $MgCl_2$ solutions than in DI water to effectively reduce the adsorption.

.

Table 6 Cations concentration in various solutions equilibrium with dolomite

| | DI | Brine | NaCl | $MgCl_2$ |
|---|---|---|---|---|
| $Al^{3+}$ (mol/L) | 0 | 0 | 0 | 0 |
| $Ca^{2+}$ (mol/L) | $6.50\times10^{-3}$ | $5.25\times10^{-1}$ | $1.36\times10^{-2}$ | $3.24\times10^{-2}$ |
| $Mg^{2+}$(mol/L) | $6.55\times10^{-3}$ | $1.26\times10^{-1}$ | $1.16\times10^{-2}$ | 1.60 |
| $Na^+$ (mol/L) | 0 | 3.12 | 5.04 | 0 |

Table 7 Cations concentration in various solutions equilibrium with kaolin

| | DI | Brine | NaCl | $MgCl_2$ |
|---|---|---|---|---|
| $Al^{3+}$ (mol/L) | $7.21\times10^{-5}$ | $5.95\times10^{-4}$ | $2.92\times10^{-4}$ | $1.21\times10^{-3}$ |
| $Ca^{2+}$ (mol/L) | 0 | $5.25\times10^{-1}$ | 0 | 0 |
| $Mg^{2+}$(mol/L) | 0 | $1.26\times10^{-1}$ | 0 | 1.69 |
| $Na^{+}$ (mol/L) | 0 | 3.12 | 5.08 | 0 |

The trivalent cations, *e.g.*, $Al^{3+}$, can reduce the adsorption more effectively per unit concentration than divalent cations. C12 solutions with various initial concentrations of $Al^{3+}$ ions were prepared by mixing C12 solutions and high concentrations of $AlCl_3$ solutions. The adsorption of C12 on silica ($SiO_2$) in DI water and brine with various initial concentrations of $Al^{3+}$ is shown in Figure 10. The adsorption was reduced from 5.33 to 4.48 mg/m$^2$ in DI water with $1.07\times10^{-4}$ mol/L $Al^{3+}$, and was reduced from 4.26 to 3.31 mg/m$^2$ in the brine with $1.51\times10^{-3}$ mol/L $Al^{3+}$, which demonstrates that $Al^{3+}$ ions are more effective for reducing the adsorption per unit cation concentration compared to the high concentrations of divalent cations in brine. However, the adsorption did not decrease with increasing initial concentrations of $Al^{3+}$, but reached constants after the initial concentrations of $Al^{3+}$ were higher than $1.07\times10^{-4}$ mol/L in DI water and $1.51\times10^{-3}$ mol/L in brine. That may be because the concentrations of $Al^{3+}$ were limited by the pH and low solubility product of $Al(OH)_3$. The solubility product of $Al(OH)_3$ at 25 °C and zero ionic strength is only $3.16\times10^{-34}$ (Butler and Cogley, 1998), which implies the highest concentration of $Al^{3+}$ that is soluble is $3.16\times10^{-4}$ mol/L in DI water at the equilibrium pH of 4. Thus, the concentration of $Al^{3+}$ in solutions has reached a limit even with higher initial concentrations, and further addition results in precipitation of aluminum hydroxide ($Al(OH)_3$).

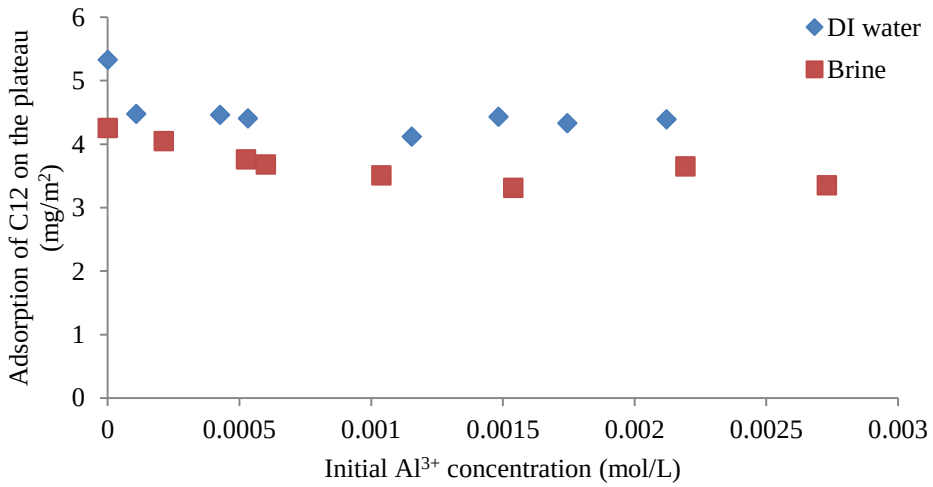


Figure 10 The adsorption of C12 on the silica ($SiO_2$) minerals with various $Al^{3+}$ concentrations

The adsorption reduction per unit cations concentration ($AR$) was defined in Equation 6 to distinguish the effect of each cations.

$$AR = \frac{adsorption\ reduction\ by\ cation\ M}{concentration\ of\ cation\ M} \qquad \textbf{Equation 6}$$

The adsorption results on silica sands are analyzed for $AR$ of various cations. $Na^+$ doesn't affect the adsorption on silica, thus $AR(Na^+) = 0$. The adsorption in NaCl solution rather than in water was used as a reference for zero $AR$ to exclude the ionic strength influence. The $AR(Mg^{2+})$, $AR(Ca^{2+})$ and $AR(Al^{3+})$ can be calculated based on Equation 7 to Equation 9.

$$AR(Mg^{2+}) = \frac{A_{NaCl} - A_{MgCl2}}{[Mg^{2+}]_{MgCl2}} \qquad \textbf{Equation 7}$$

$$AR(Ca^{2+}) = \frac{A_{NaCl} - A_{brine} - [Mg^{2+}]_{brine} \times AR(Mg^{2+})}{[Ca^{2+}]_{brine}} \qquad \textbf{Equation 8}$$

$$AR(Al^{3+}) = \frac{A_{brine} - A_{brine+AlCl3}}{[Al^{3+}]_{brine+AlCl3}} \qquad \textbf{Equation 9}$$

where $A$ indicates the adsorption; the subscript $NaCl$, $MgCl2$, and $brine$ indicate the corresponding aqueous solution as listed in Table 5; the subscript $brine + AlCl3$ indicates the brine solution with $1.51\times10^{-3}$ mol/L $Al^{3+}$.

The effect of each cation for reducing adsorption on silica is quantitatively described by $AR$, as compared in Figure 11. $Al^{3+}$ is most effective for adsorption reduction per unit cation concentration.

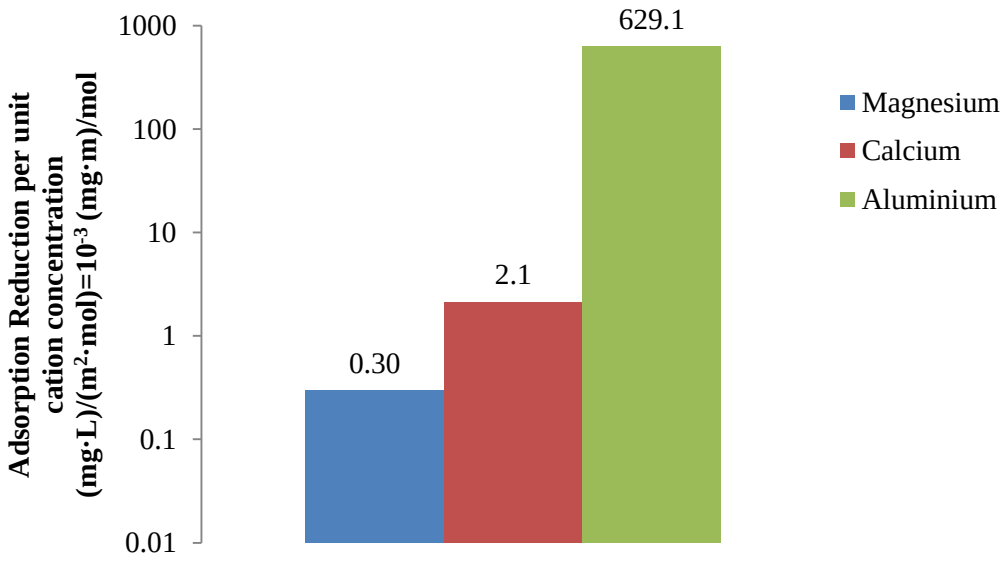


Figure 11 The adsorption reduction per unite cation concentration

**Adsorption of C12 on Formation Minerals**

Adsorption measurements of C12 were made on a potential formation for $CO_2$ EOR. X-ray diffraction study of three core plug samples was carried out to examine their mineralogy. Analysis of these patterns indicates that the samples are composed of mainly calcite. Quantitative phase analysis of XRD diffraction pattern for these samples revealed that the three core plugs were composed of 95.4 - 98.6% Calcite, 0.5 - 4.1% Dolomite, and 0.4 - 0.9% Quartz.

The BET surface area of the cores samples is 4.00 $m^2/g$. The results in Figure 11 indicate that the adsorption of C12 in synthetic brine is low on this formation material which has low quartz content.

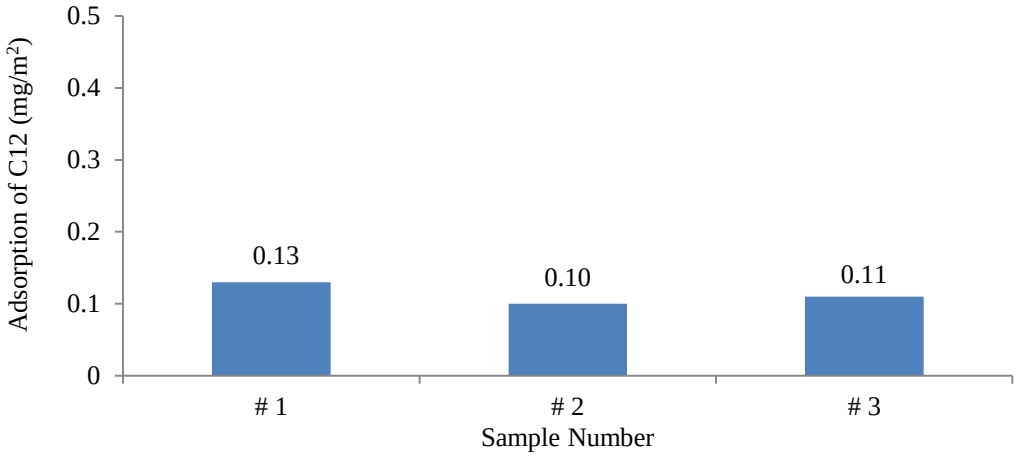


Figure 11 The adsorption of C12 in synthetic brine on the formation minerals.

**Conclusions**

The adsorption of cationic surfactants in carbonate reservoirs is expected to be low during $CO_2$ flooding with foam mobility control processes, because of the expected positive surface charge of carbonate minerals at the low pH of $CO_2$ flooding. However, the silica and clay impurities with negatively charged binding sites can adsorb significant amount of cationic surfactants and cause the high adsorption of cationic surfactants on some natural carbonate minerals.

The amount of adsorption of cationic surfactant on minerals is expected to depend on the surface charge of the mineral. The isoelectric divalent ion concentration, $[Me^{2+}]^*$ was proposed for determining the sign of the surface charge. If the $Me^{2+}$ activity of the brine are greater than the isoelectric $[Me^{2+}]^*$ concentration, then the surface charge should be positive and the adsorption of cationic surfactant is expected to be low on the pure mineral surface. If the $Me^{2+}$ activities of the brine are less than the isoelectric $[Me^{2+}]^*$ concentrations, then the opposite is expected.

The adsorption of the switchable cationic surfactants, *e.g.*, Ethomeen C12, can be reduced by the presence of multivalent cations in the brine. The adsorption of C12 on silica was reduced from 5.33 $mg/m^2$ in DI water to 3.31 $mg/m^2$ in synthetic brine with $1.51\times10^{-3}$ mol/L $Al^{3+}$. The effectiveness of cations for reducing adsorption ranges in the order of: $Al^{3+}>Ca^{2+}>Mg^{2+}$. However, the low concentrations of $Al^{3+}$ in solutions caused by low solubility product of aluminum hydroxide ($Al(OH)_3$) limit the benefit of $Al^{3+}$ for reducing adsorption.

The adsorption of C12 in synthetic brine is low on formation mineral which contains low quartz content.

**Acknowledgements**

We acknowledge financial support from the Abu Dhabi National Oil Company (ADNOC), the Abu Dhabi Oil R&D Sub-Committee, Abu Dhabi Company for Onshore Oil Operations (ADCO), Zakum Development Company (ZADCO), Abu Dhabi Marine Operating Company (ADMA-OPCO) and the Petroleum Institute (PI), U.A.E and partial support from the US Department of Energy (under Award No. DE-FE0005902).

**References**

Alkan, M., Demirbaş , Ö. and Doğan, M. 2005. Electrokinetic properties of kaolinite in mono- and multivalent electrolyte solutions. *Microporous and Mesoporous Materials,* **83**(1-3), 51–59.

Butler, J. and Cogley, D. 1998. *Ionic Equilibrium: Solubility and pH Calculations.* Canada: John Wiley & Sons, Inc.

Chen, Y., Elhag, A. S., Poon, B. M., Cui, L., Ma, K., Liao, S. Y., Reddy, P. P., Worthen, A. J., Hirasaki G. J., Nguyen, Q. P., Biswal, S. L. and Johnston, K. P. 2014. Switchable Nonionic to Cationic Ethoxylated Amine Surfactants for $CO_2$ Enhanced Oil Recovery in High-Temperature, High-Salinity Carbonate Reservoirs. *SPE Journal.* Preprint: SPE-154222-PA.

de Souza, A. V. O. and Fjelde I. 2013. Modeling of Interaction Between $CO_2$ and Rock in Core Flooding Experiments. Presented at SPE Heavy Oil Conference-Canada, 11-13 June, Calgary, Alberta, Canada.

Farajzadeh, R., Andrianov, A. and Zitha, P. 2010. Investigation of Immiscible and Miscible Foam for Enhancing Oil Recovery. *Ind. Eng. Chem. Res.*, 1910-1919.

Foxall, T., Peterson, G., Rendall , H. and Smith , A. 1979. Charge determination at calcium salt/aqueous solution interface. *Journal of the Chemical Society, Faraday Transactions 1: Physical Chemistry in Condensed Phases,* **75**, 1034-1039.

Hanssen, J. and Surguchev, L. 1994. Foam Processes: An Assessment of Their Potential in North Sea Reservoirs Based on a Critical Evaluation of Current Field Experience. Presented at SPE/DOE Improved Oil Recovery Symposium. Tulsa, Oklahoma: Society of Petroleum Engineers.

Hao, Y., Wu, Z., Ju, B., Chen, Y. and Luo, X. 2004. Laboratory Investigation of $CO_2$ Flooding. Presented at Nigeria Annual International Conference and Exhibition,. Abuja, Nigeria: Society of Petroleum Engineers.

Heberling, F., Trainor, T., Lützenkirchen, J., Eng, P., Denecke, M. and Bosbach, D. 2011. Structure and reactivity of the calcite–water interface. *Journal of Colloid and Interface Science,* **342**(2), 843-857.

Hirasaki, G. J. and Zhang, D. L., 2004. Surface chemistry of oil recovery from fractured, oil-wet, carbonate formations. *SPE J.*, **9**(2), 151-162.

Kielland, J. 1937. Individual activity coefficients of ions in aqueous solutions. *Journal of the American Chemical Society,* **59**, 1675-1678.

Kosmulski, M. 2003. A literature survey of the differences between the reported isoelectric points and their discussion. *Colloids and Surfaces A: Physicochemical and Engineering Aspects,* **222**(1-3), 113–118.

Liu, Y., Grigg, R., and Bai, B. 2005. Salinity, pH , and Surfactant Concentration Effects on $CO_2$-Foam. Presented at SPE International Symposium on Oilfield Chemistry. The Woodlands, Texas: Society of Petroleum Engineers.

Ma, K., Cui, L., Dong, Y., Wang, T., Da, C., Hirasaki, G. and Biswal, S. 2013. Adsorption of cationic and anionic surfactants on natural and synthetic carbonate materials. *J Colloid Interface Sci,* **408**, 164–172.

Mannhardt, K., Schramm, L. and Novosad, J. 1993. Effect of Rock Type and Brine Composition on Adsorption of Two Foam-Forming Surfactants. *SPE Advanced Technology Series,* **1**(1), 212-218.

Moradi-Araghi, A., Johnston, E., Zornes, D. and Harpole, K. 1997. Laboratory Evaluation of Surfactants for $CO_2$-Foam Applications at the South Cowden Unit. Presented at International Symposium on Oilfield Chemistry. Houston, TX: Society of Petroleum Engineers.

Pokrovsky, O., Schott, J. and Thomas, F. 1999. Dolomite surface speciation and reactivity in aquatic systems. *Geochimica et Cosmochimica Acta*, **63**(19-20), 3133–3143.

Sammalkorpi, M., Karttunen, M. and Haataja, M. (2009). Ionic surfactant aggregates in saline solutions: sodium dodecyl sulfate (SDS) in the presence of excess sodium chloride (NaCl) or calcium chloride (CaCl2). *The Journal of Physical Chemistry B,* **113**(17), 5863-5870.

Sánchez-Martín, M., Dorado, M., del Hoyo, C. and Rodríguez-Cruz, M. 2008. Influence of clay mineral structure and surfactant nature on the adsorption capacity of surfactants by clays. *Journal of Hazardous Materials*, **150**(1), 115-123.

Sanders, A., Jones, R., Linroth, M. and Nguyen, Q. 2012. Implementation of a $CO_2$ Foam Pilot Study in the SACROC Field: Performance Evaluation. Presented at SPE Annual Technical Conference and Exhibition. San Antonio, Texas, USA: Society of Petroleum Engineers.

Sequeira, D., Ayirala, S. and Rao, D. 2008. Reservoir Condition Measurements of Compositional Effects on Gas-Oil Interfacial Tension and Miscibility. Presented at SPE/DOE Symposium on Improved Oil Recovery. Tulsa, Oklahoma, USA: Society of Petroleum Engineers.

Shedid, S., Zekri, A. and Almehaideb, R. 2007. Laboratory Investigation of Influences of Initial Oil Saturation and Oil Viscosity on Oil Recovery by $CO_2$ Miscible Flooding. Presented at EUROPEC/EAGE Conference and Exhibition. London, U.K.: Society of Petroleum Engineers.

Somasundaran, P. and Agar, G. 1967. The zero point of charge of calcite. *Journal of Colloid and Interface Science*, **24**(4), 433–440.

Stephenson, D., Graham, A. and Luhning, R. 1993. Mobility Control Experience in the Joffre Viking Miscible $CO_2$ Flood. *SPE Reservoir Engineering*, **8**(3), 183-188.

Stevens, J., Martin, F. and Harpole, K. (1995). $CO_2$ Foam Field Verification Pilot Test at EVGSAU: Phase IIIB--Project Operations and Performance Review. *SPE Reservoir Engineering*, **10**(4), 266-272.

Tabatabal, A., Gonzalez, M. V., Harwell, J. H. and Scamehorn, J. F. 1993. Reducing Surfactant Adsorption in Carbonate Reservoirs. *SPE Reservoir Engineering*, **8**(2), pp. 117 - 122.

Talebian, S., Masoudi, R., Tan, I. and Zitha, P. 2013. Foam assisted $CO_2$-EOR; Concepts, Challenges and Applications. Presented at SPE Enhanced Oil Recovery Conference. Kuala Lumpur, Malaysia: Society of Petroleum Engineers.

Thibaut, A., Misselyn-Bauduin, A., Grandjean, J., Broze, G. and Jérôme, R. 2000. Adsorption of an Aqueous Mixture of Surfactants on Silica. *Langmuir*, **16**(24), 9192–9198.

Tombácz, E. and Szekeres, M. 2006. Surface charge heterogeneity of kaolinite in aqueous suspension in comparison with montmorillonite. *Applied Clay Science*, **34**(1-4), 105-124.

Tsau, J. and Heller, J. 1992. Evaluation of Surfactants for $CO_2$-Foam Mobility Control. Presented at Permian Basin Oil and Gas Recovery Conference. Midland, Texas: Society of Petroleum Engineers.

Vdović, N. 2001. Electrokinetic behaviour of calcite—the relationship with other calcite properties. *Chemical Geology*, **177**(3-4), 241–248.

Zhang, R. and Somasundaran, P. 2006. Advances in adsorption of surfactants and their mixtures at solid/solution interfaces. *Advances in Colloid and Interface Science*, **123**, 213–229.